https://doi.org/10.1007/s41230-021-1073-z

Effect of mould baffle technology on stray grain formation in single crystal blades by integral fabrication based on 3D printing

**Zhe-feng Liu, **Kai Miao, Wei-bo Lian, *Zhong-liang Lu, Chen Yi and Di-chen Li

State Key Laboratory of Manufacturing Systems Engineering, School of Mechanical Engineering, Xi'an Jiaotong University, Xi'an 710049, China

Abstract: Stray grains, the most serious casting defect, mainly occur in the platform because of the abrupt transition of the cross-section in the directional solidification of superalloy single-crystal blades. A new mould baffle technology based on 3D printing and gelcasting is proposed herein to reduce the formation of stray grains in the platform. The influence of the proposed mould baffle technology on the temperature field in the platform during solidification was investigated by simulation and experiment. The numerical simulation results indicate that the proposed mould baffle technology can effectively hinder the radiation and heat dissipation at the platform extremities, and therefore, reduce undercooling in the platform and the formation of stray grains during directional solidification. Casting trials of a hollow turbine blade were conducted using CMSX-4 superalloy. The trial results demonstrate the potential of the proposed approach for manufacturing single-crystal superalloy blades.

Key words: single crystal; directional solidification; stray grains; temperature field; numerical simulation

CLC numbers: TG146.1$^+$5 **Document code:** A **Article ID:** 1672-6421(2021)05-433-09

1 Introduction

Single-crystal (SC) superalloy blades have good durability, low creep rates, and excellent thermal fatigue resistance because of the lack of high-temperature weak grain boundary structure. For this reason, they are widely used in advanced aero-engine and gas turbine engines [1-2]. The manufacture of SC superalloy blades is based on directional solidification (DS). During DS, a shell mould with alloy melt is withdrawn from a heating zone into a cooling zone, and this leads to the formation of an SC structure from the bottom to the top of the blade. However, casting defects such as stray grains may occur because unidirectional heat flux cannot be guaranteed, or the temperature gradient is inadequate to cause local undercooling. As the most serious type of casting defect, stray grains are mainly formed on the platform because of the abrupt transition of the cross section and rapid cooling of the local melt. Due to the large radiation angle at the extremities of the platform, the temperature drops rapidly during DS, leading to the formation of a supercooled region that promotes stray grains the nucleation and growth. Stray grains destroy the integrity of the SC and degrade its mechanical properties owing to the introduction of new grain boundaries. Moreover, large-angle grain boundaries are formed between the stray grains and the SC matrix. Many impurities and brittle phases aggregate in these large-angle grain boundary regions at the end of solidification, and cracks originate from these regions during blade service, which severely reduce the fatigue life of blades [3]. Therefore, it is important to eliminate and control the formation of stray grains at the extremities of the platform during the manufacture of SC blades.

To prevent the formation of stray grains in the solidification process, many researchers have attempted to suppress the nucleation of stray grains by improving the local temperature field. It is believed that a hot spot is caused by the poor cooling condition in the geometric structure transition zone between the platform and the blade body, where the alloy melt remains overheated

*Zhong-liang Lu

Professor and Doctoral Supervisor. Prof. Lu focuses his research on 3D printing principles, technology and application. He has presided over or participated in a series of projects funded by the National Natural Science Foundation of China, National Key R & D Program, and National Active & Standby Machine Project. To date, he has published more than 90 academic papers, three monographs on 3D printing, and possesses more than 50 invention patents of China. Prof. Lu is a Senior Member of Chinese Mechanical Engineering Society and a Senior Member of Additive Manufacturing and 3D Printing Institution.

E-mail: zllu@mail.xjtu.edu.cn

**Zhe-feng Liu and Kai Miao contribute equally to this article and should be considered co-first authors.

Received: 2021-05-31; Accepted: 2021-09-24

for an extended period and retards SC growth from the blade body to the undercooled platform. This is the main reason for the formation of stray grains at the platform extremities. A series of methods has been used to weaken the heat barrier with the aim of promoting SC growth from the blade body or prolong the nucleation time by reducing the undercooling. Ma et al. [4-6] attached a graphite block with high thermal conductivity adjacent to the hotspot region to minimize the heat barrier by enhancing local heat conduction. Meyer et al. [7] attempted to impede local cooling of the alloy melt by placing heat insulation material at the platform extremities to ensure that the SC branches have adequate time to fill up the platform before the occurrence of undercooled nucleation. The grain continuator (GC) technique is often employed to avoid the heat barrier zone in the DS of large blades such as gas turbine blades. A continuator can be established for transferring the SC from the blade body to the platform extremities. However, subgrain boundaries are easily formed between the dendrite arms in the continuator and those in the blade section, and they sharply degrade the mechanical properties of the casting. Yang et al. [8] controlled the formation of stray grains by momentarily decreasing the drawing rate to minimize the curvature of the isotherm in the platform, which weakened the "hotspot" effect and reduced undercooling. The above research results provide a deep interpretation of the formation mechanism of stray grains on the platform of the SC blade. However, these methods are overly complex and do not facilitate mass production. Moreover, these methods are mainly guided by experience and lack an accurate design.

During DS, the ceramic mould greatly influences heat dissipation of the casting. A reasonable ceramic mould design can improve the local temperature field. For example, one can change the wall thickness of the mould to adjust the heat dissipation rate. However, in the traditional investment casting process, the mould structure is limited by the die, and it is difficult to flexibly design a complex mould structure. Wu et al. [9-11] proposed the integral fabrication technique of ceramic mould (IFTCM) based on three-dimensional (3D) printing and ceramic gelcasting to facilitate the fabrication of ceramic parts with complex internal cores. Giving full play to 3D printing technology, a mould with a complex structure can be manufactured with efficient and low-cost by IFTCM, without being constrained by the die. Thus, a shell mould with any reasonable external structure can be manufactured considering its heat dissipation needs. This technique represents a new approach to eliminating casting defects by altering the mould structure in relation to heat dissipation during DS. Based on the above considerations, a new mould baffle technology based on IFTCM is proposed to eliminate the casting defect of stray grains in SC blades. Based on 3D printing technology, a specific baffle is easily "added" to the mould to alter the heat radiation on the platform to reduce undercooling and eliminate the formation of stray grains. The effect of the proposed mould baffle technology on the temperature field at the platform extremities is investigated by conducting a simulation and an experiment. The alloy material used in this study is CMSX-4 superalloy. The results of the present study are expected to promote the application of mould baffle technology in the fabrication of SC blades and provide a better understanding of the formation mechanism of stray grains in the platform of SC blades.

2 Experimental procedure

2.1 Ceramic mould preparation

A simplified blade model consisting of a grain selector, blade body, platform, and tenon is designed for numerical simulation, as shown in Fig. 1. Notably, the research object of this study is the platform, therefore, the structure of other parts of the blade is simplified in the simulation process to reduce unnecessary calculations. The thickness of the platform is 2 mm, and the maximum length of the platform is 10 mm. To reduce the undercooling caused by rapid heat dissipation of the alloy melt

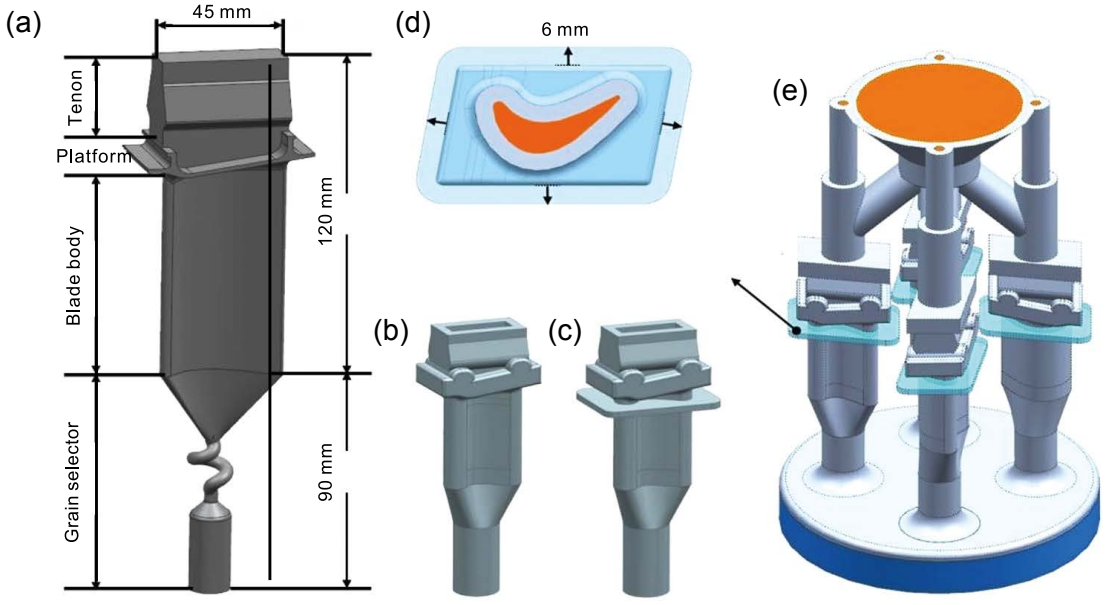

Fig. 1: Blade structure (a), traditional mould (b), improved mould (c), mould baffle (d), and assembly moulds (e)

at the platform extremities during DS, the shell mould was improved by introducing a mould baffle under the platform, as shown in Fig. 1(c). Considering the effect of the baffle on radiation shielding and the difficulty of manufacturing, the mould baffle was designed based on the contour of the platform, offset by 6 mm, with a thickness of 5 mm, and 5 mm below the platform, as shown in Fig. 1(d). The wall thickness of the shell mould was set to 7 mm considering its comprehensive strength requirements. Then, the moulds were assembled in groups of four and placed on a water-cooled copper plate. The casting system included the blade mould with the proposed baffle, centre support rod, bottom plate, and gating and risering system, as shown in Fig. 1(e).

The detailed procedures for manufacturing the ceramic mould by means of 3D printing and gelcasting are shown in Fig. 2(a). Resin prototypes were fabricated using a stereolithography (SL) rapid prototyping machine (SPS600B, Xi'an Jiaotong University, China) and photosensitive resin (SPR 8981, Zhengbang Technology Co. Ltd., China). Commercial alumina powders with four different particle sizes, i.e., 100, 40, 5, and 2 μm (Shandong Zibo Aluminum, Inc., China), were adopted to build the ceramic matrix. The reagents used for gelcasting are listed in Table 1. Then, an alumina matrix ceramic slurry with high solid loading (60vol.%) was prepared by means of ball-milling for 40 min to be used in the gelcasting process. The ceramic slurry, which had a viscosity of less than 1 Pa·s, was poured into the SL prototype and polymerized to form a green body under the effect of the initiator and catalyst. Subsequently, the green ceramic mould was vacuum freeze-dried for 24 h to reduce shrinkage and avoid drying-related cracks [12]. Finally, the integral ceramic mould was obtained after presintering and post-treatment [13-15]. Both the traditional mould and the improved mould with the mould baffle were prepared under the same conditions for comparison, as shown in Figs. 2(b, c).

Table 1: Reagents used for gelcasting

Reagents	Function
Acrylamide (AM)	Monomer
N, N' - methylene diacrylamide (MBAM)	Cross-linker
N, N, N', N' - tetramethylethylenediamine	Catalyst
Ammonium persulfate	Initiator
Sodium polyacrylate	Dispersant
Deionized water	Solvent
Strong ammonia	pH adjuster

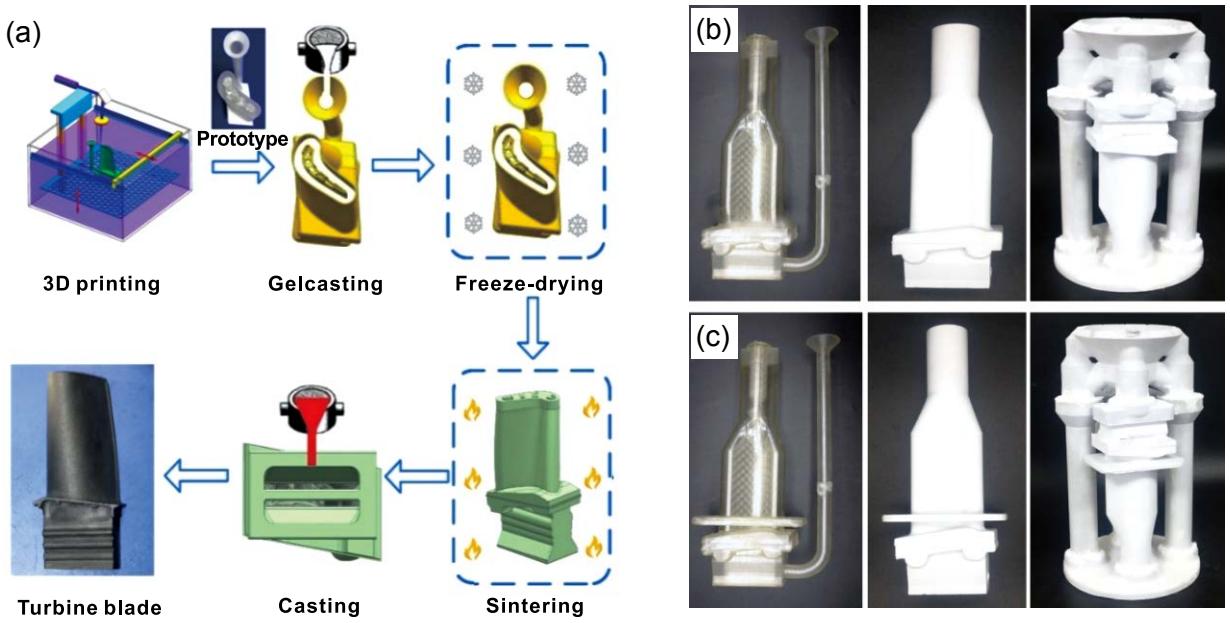

Fig. 2: IFTCM process (a) and traditional (b) and improved (c) moulds

2.2 Finite element modelling and analysis

To analyze the influence of the proposed mould baffle technology on the DS process, the temperature distribution, temperature gradient, solidification rate, and shape of liquidus isotherm of the blade were numerically simulated by using the finite element analysis (FEA) software application ProCAST. The traditional and improved models were simulated under the same conditions for comparison. A 1/4 model was employed to improve the calculation efficiency in the simulation, as shown in Fig. 3. It was assumed that heat exchange between the DS furnace wall and the ceramic shell mould surface occurred through radiation during DS due to the vacuum environment. The key simulation parameters are summarized in Table 2.

2.3 Casting

CMSX-4 nickel superalloy was used as the experimental material for casting, and its main chemical compositions are listed in Table 3.

A three-chamber vacuum DS furnace (ZGD-20B, Hangxing Vacuum Equipment Co., Ltd., China) was used to cast the

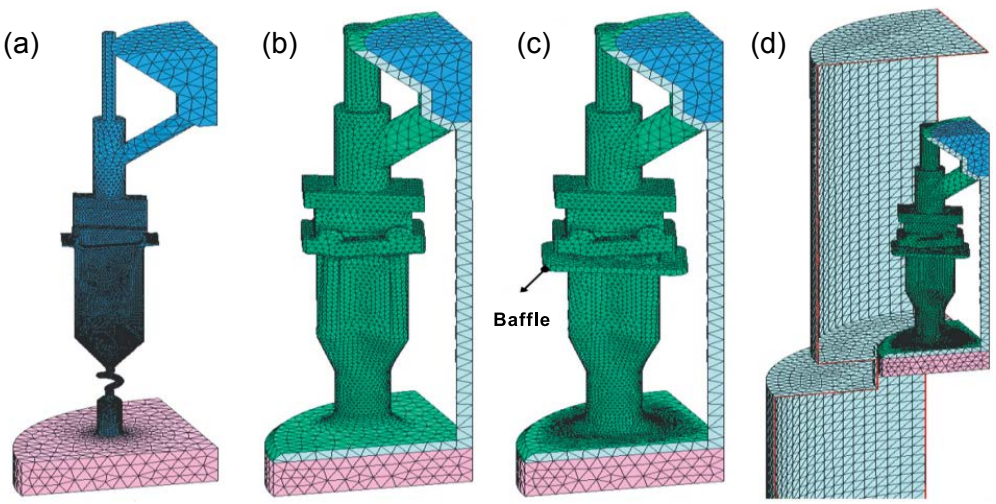

Fig. 3: Grid model of casting system: blade (a); traditional mould (b); improved mould (c); and directional solidification system (d)

Table 2: Key parameters of ProCAST-based numerical simulation

Parameters	Value
Heating zone temperature	1,550 °C
Transition zone temperature	1,000 °C
Cooling zone temperature	50 °C
Crystallizer temperature	50 °C
Thermal radiation coefficient (hot and cool zones)	0.8 [16]
Thermal radiation coefficient (transition zone)	0.8 [16]
Thermal radiation coefficient (shell mould)	0.7
Heat transfer coefficient (water-cooled ring/metal)	2,000 $W \cdot m^{-2} \cdot K^{-1}$ [17]
Heat transfer coefficient (mould/metal)	500 $W \cdot m^{-2} \cdot K^{-1}$ [17]
Heat transfer coefficient (water-cooled ring/mould)	20 $W \cdot m^{-2} \cdot K^{-1}$ [17]

Table 3: Chemical composition of CMSX-4 superalloy (wt.%)

Cr	Mo	Co	W	Ta	Al	Ti	Hf	Re	Ni
6.4	0.61	9.6	6.4	6.6	5.67	1.04	0.1	2.9	60.68

SC blade. This furnace is based on the well-known Bridgman process, as shown in Fig. 4. As reported by Chapman et al.[18], the liquidus of CMSX-4 nickel superalloy is 1,382 °C. In the DS process, the shell mould was preheated to 1,550 °C, and the CMSX-4 superalloy melt was poured into the mould at the same temperature and held for approximately 5 min. During this time, the liquid metal at the bottom of the shell starts to nucleate and grow under the chilling effect of the water-cooled crystallizer. Subsequently, the mould containing the alloy melt was pulled down from the heating zone to the cooling zone at constant pulling rates of 1, 3, and 5 $mm \cdot min^{-1}$, respectively. A unidirectional temperature gradient was formed in the molten metal, and the solidification structure started to grow directionally until the metal completely solidified. Finally, the SC structure was obtained.

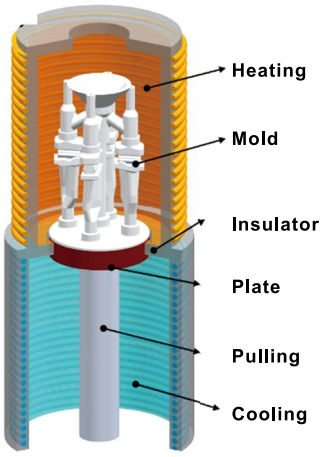

Fig. 4: Schematic diagram of DS furnace

To study the influence of different baffle sizes on the formation of stray grains in the platform, taking the standard mould as the reference group, moulds with different baffle sizes were designed as the comparison group. By using finite element models, the temperature field distribution and microstructure evolution process of the DS process were investigated by conducting a combined temperature field simulation and CAFE grain simulation. The thermophysical parameters were automatically calculated using ProCAST software for the material composition given in Table 3.

The heating zone of the DS equipment consisted of a graphite heater with a diameter of 400 mm and height of 500 mm. The diameter of the cooling zone was 500 mm. The heating and cooling zones were isolated from each other by an insulator. The diameter of water-cooled copper plate used to fix the mould was 250 mm.

3 Results and discussion

3.1 Calculation results

To verify the superiority of the proposed mould baffle technology, the improved mould with the mould baffle and the traditional mould were compared under the same conditions in the simulation conducted herein. The change in temperature field during DS governed the formation of the isolated undercooling region in the platform. When the degree of undercooling of the isolated undercooling region approached the critical nucleation undercooling of the alloy, the probability of stray grain formation was high [19]. The difference between the temperature distributions in the shell mould and the blades is shown in Fig. 5. As the platform transitions to the cooling zone from the heating zone, the isolated undercooling region starts to form at the platform extremities.

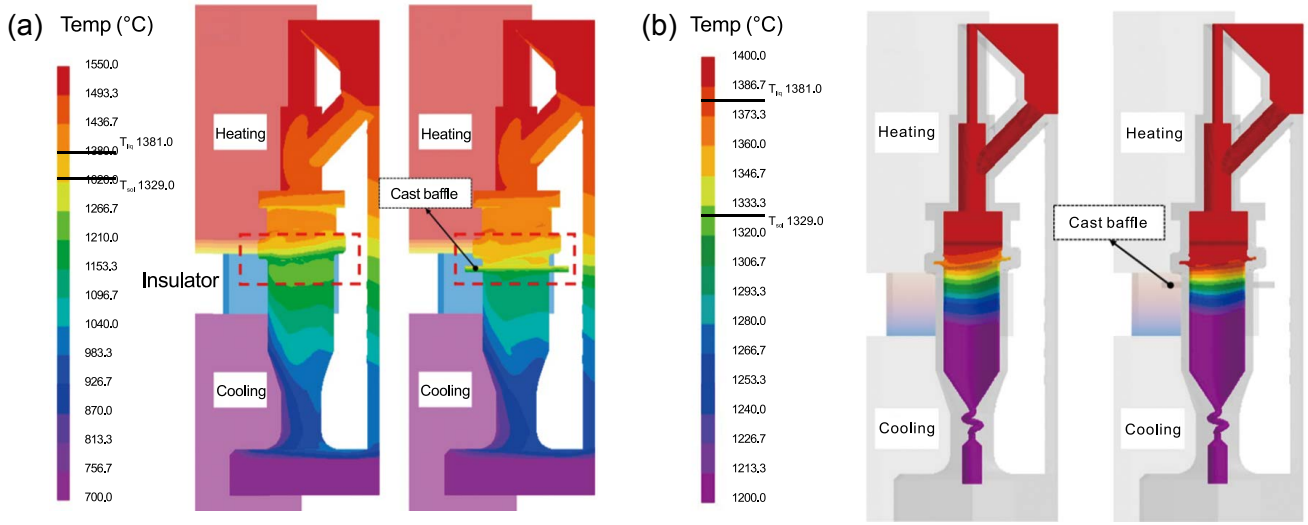

Fig. 5: Comparison of temperature fields in moulds (a) and blades (b) when displacement is 170 mm and drawing rate is 3 mm·min^{-1}

As shown in Fig. 5, when the casting descends by 170 mm at the drawing rate of 3 mm·min^{-1}, the platform of the blades approaches the insulator. The temperature of the platform extremities of the traditional mould (approximately 1,200 °C) is considerably lower than that of the improved mould with the mould baffle (approximately 1,300 °C), as shown in Fig. 5(a). Accordingly, the temperature at the platform extremities of the blade cast using the traditional mould is approximately 80 °C lower than that of the blade cast using the improved mould. Therefore, the improved mould with the mould baffle can reduce undercooling of the alloy melt at the platform extremities.

To evaluate the effect of the proposed mould baffle technology on the solidification of alloy melt at the platform extremities, two points in the platform with the greatest temperature difference between them were selected for comparison to explain whether critical undercooling would occur. Points A and B were located at the tip angle of the platform and joint position of the blade body and platform, respectively, as shown in Fig. 6(a). The temperature difference curves of the two points under different drawing rates during DS are shown in Fig. 6(b). Curves 1, 2, and 3 indicate the variation of temperature difference [temp (A−B)] between Points A and B with displacement of the improved mould, and Curves 4, 5, and 6 indicate the same for the traditional mould; in both cases, the drawing rates are 1, 3, and 5 mm·min^{-1}, respectively. The horizontal axis represents the displacement of the casting, which is obtained by multiplying the drawing rate and the drawing time, and the vertical axis represents the temperature difference between Points A and B. Theoretically, the greater the temperature difference between Points A and B, the higher the occurrence probability of undercooled nucleation, which leads to the formation of stray grains at Point A.

Between the two vertical lines lies the 25 mm range that corresponds to the time before and after the platform passes through the insulator. Stray grains in the platform are usually formed in this range. When the temperature difference [temp (A−B)] > 0, Point B solidifies before Point A, it means that undercooled nucleation does not occur at Point A, that is, no

stray grains are generated. By contrast, when [temp (A–B)] < 0, Point A solidifies before Point B, it means that undercooled nucleation possibly occurs at Point A; therefore, stray grains may be formed at Point A. The greater the value of [temp (A–B)], the lower the probability of stray gain formation at Point A. A faster drawing rate reduces the temperature difference between Points A and B during the solidification process and increases the probability of stray grain formation. For all drawing rates, in case of the improved mould, the temperature difference between Points A and B is significantly higher than that in case of the traditional mould. Therefore, the prediction is that the improved mould with the proposed mould baffle can greatly reduce the probability of stay grain formation in the platform. When the drawing rate is 1 mm·min^{-1}, as shown in Fig. 6(b), the temperature of Point A is higher than that of Point B across the entire 25 mm region, and the probability of stray grain formation in the platform is eliminated.

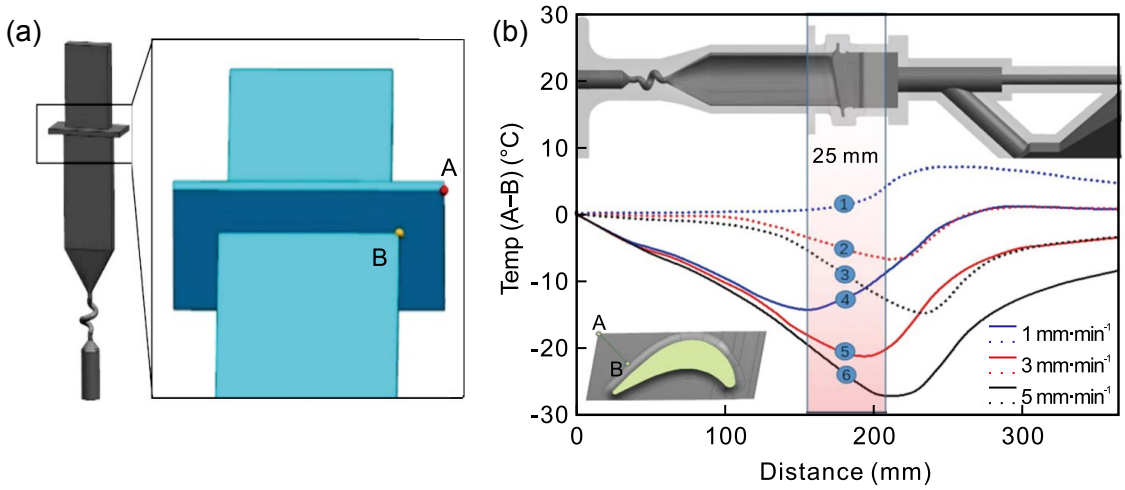

Fig. 6: Location of Points A and B (a), and temperature difference between Points A and B at drawing rates of 1, 3, and 5 mm·min^{-1} (b)

To determine the optimal baffle size by considering the maximum vertical profile of the platform, the distance (Δx) was adjusted outward, as shown in Fig. 7. Then, six moulds with different baffle sizes were designed, where the values of Δx were –4 mm, –2 mm, 0 mm, 2 mm, 4 mm, and 6 mm. The mesh models of the moulds with different baffle sizes are shown in Fig. 7(a). The temperature field and grain growth during the DS process were simulated at the drawing rate of 5 mm·min^{-1}.

The variation of temperature difference between Points A and B [temp (B–A)] for different baffle sizes is shown in Fig. 7(b). The greater the value of [temp (B–A)], the higher the occurrence probability of undercooled nucleation. The value of [temp (B–A)] decreases as the baffle size increases. When Δx is 6 mm, the temperature of Point B is always lower than that of Point A, meaning that undercooled nucleation cannot occur.

The results of a CAFE simulation of the grain structure in the platform formed using moulds with different baffle sizes are shown in Fig. 8. As the baffle size increases, the number and volume of stray grains in the platform decrease. When Δx increases to 6 mm, the CAFE simulation results indicate that the stray grains disappear completely, which agrees well with the previous analysis of the temperature field. Further increasing the baffle size will increase the space occupied by the casting

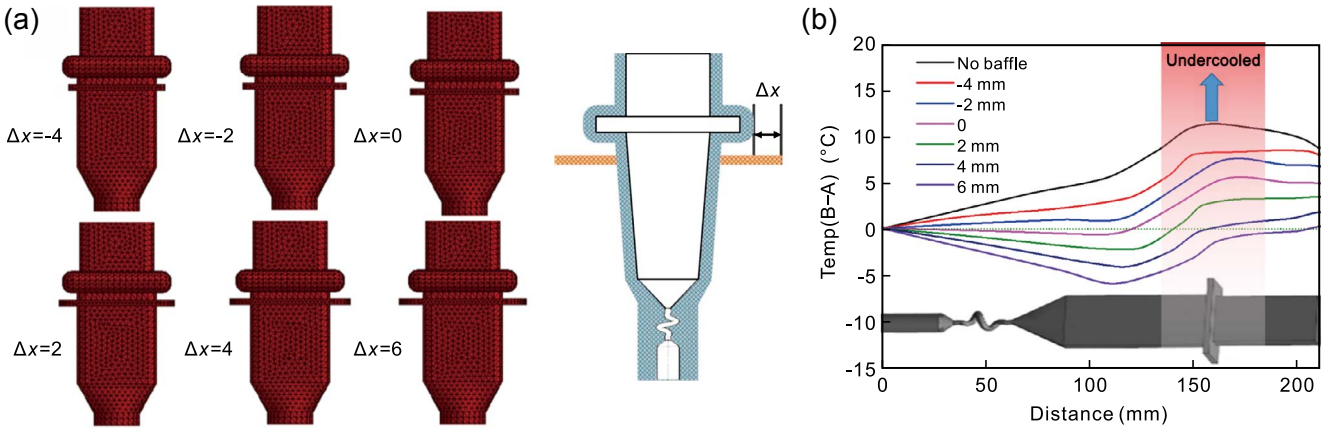

Fig. 7: Mesh models of mould with different baffle sizes (a), and temperature difference between Points B and A for different baffle sizes (b)

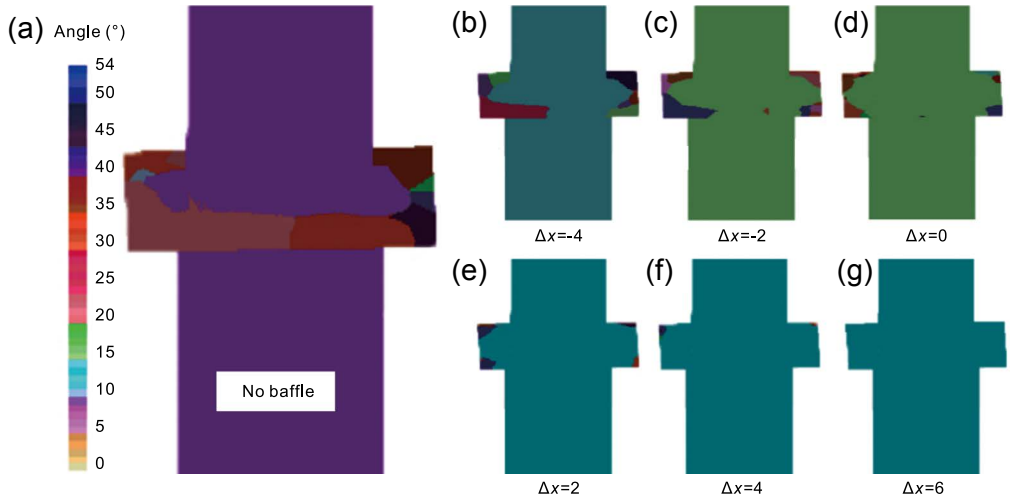

Fig. 8: Results of CAFE simulation of grain structure with different baffle sizes

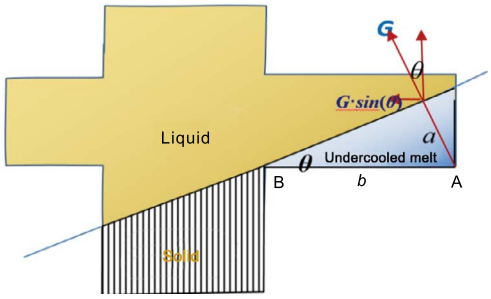

Fig. 9: Schematic diagram of stray grain formation

system and the manufacturing cost. Therefore, Δx=6 mm is optimal for the blade manufactured in this study.

3.2 Mechanism analysis

The formation positions of the stray grains are shown in Fig. 9. Because of the imbalance of the solidification interface, the melt at Point A was undercooled. When the undercooling ΔT_A at Point A satisfies Eq. (1), stray grains are formed at Point A.

$$\Delta T_A > \Delta T_{nucl} \quad (1)$$

$$\Delta T_A = G \cdot \sin\theta \cdot b \quad (2)$$

where ΔT_A denotes the undercooling at Point A, and ΔT_{nucl} denotes the critical undercooling of the alloy; G denotes the temperature gradient, θ denotes the angle between the normal of the liquidus and the gravity line, and b is the size of the platform beyond the blade body.

To explain the effect of the proposed mould baffle technology in terms of eliminating undercooled nucleation, an analysis was performed of the heat exchange process in the platform during DS. When the platform reaches a position at which it is horizontally aligned with the insulator in the DS furnace, as shown in Fig. 10(a), the influence of the hot zone on the mould temperature gradually decreases, and radiation heat exchange between the shell mould and the water-cooled ring below the insulator becomes dominant. Compared to Position B, Position A is closer to the water-cooled ring and has a larger radiation angle; therefore, the temperature of the alloy melt at the Position A decreases at a considerably higher rate, which leads to the formation of a concave solid-liquid interface, as shown in Fig. 10(b). Undercooled melt is formed at Point A owing to the high cooling rate. If the undercooling exceeds the critical undercooling before the SC branches arrive at the platform from the blade body, Eq. (1) is satisfied, and stray grains are formed.

According to Eq. (2), the undercooling ΔT_A increases as the values of θ and b increase. Normally, as the drawing rate increases, the decrease rate of the temperature at Point A is higher than that of Point B, and the concavity of the solid-liquid interface is higher [20]. Moreover, as the value of θ increases, the platform size and the value of b increase. Therefore, stray grains

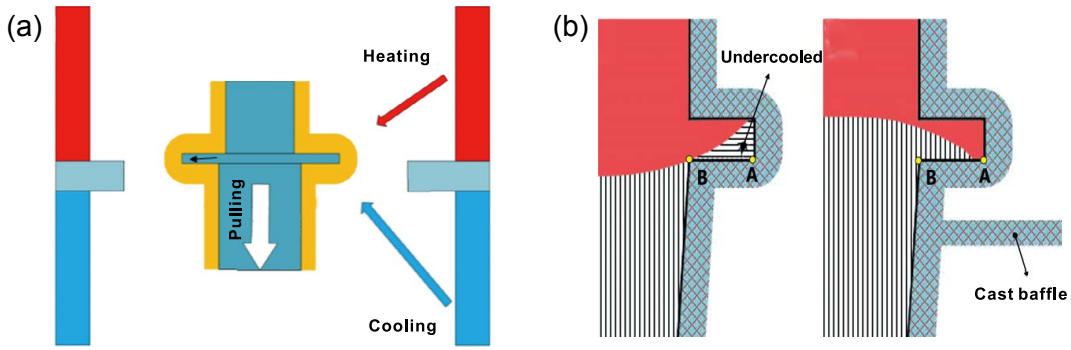

Fig. 10: Schematic diagram of heat exchange between platform and furnace (a), and effect of mould baffle on solid-liquid interface (b)

are often formed in the platform when the platform size is large or the drawing rate during DS is high. In case of the improved mould, by setting a baffle under the platform, one can block heat dissipation from the platform extremities to the cooling zone, which greatly reduces the cooling rate of the alloy melt in this region. Therefore, the original SC branches have sufficient time to arrive at the platform extremities before the formation of undercooled melt. Due to slow heat dissipation in the platform, the solidification front in the platform tends to be horizontal or "convex", as shown in Fig. 10(b). This "convex" morphology can effectively prevent the generation of stray grains [21]. In this way, the heat dissipation behavior in the platform is altered by the mould baffle. The calculation of the undercooling ΔT_A no longer obeys Eq. (2). Even if the platform size is large, the proposed mould baffle technology can successfully prevent the formation of stray grains. Moreover, an appropriate drawing rate can be set considering production efficiency, and it is not necessary to greatly reduce the drawing rate to avoid the formation of the stray grains, as is required in case of the traditional mould.

4 Trial casting

The casting experiments were conducted by setting the drawing rate to 3 mm·min^{-1} and the holding and pouring temperatures to 1,550 °C. Figure 11 shows the blades obtained after cleaning and removing surface corrosion. In the case of the blade manufactured using the traditional mould, stray grains are formed at the platform extremities [Fig. 11(b)]. By contrast, the SC structure is well maintained in the blade manufactured using the improved mould, and there are no stray grains in the platform, as shown in Fig. 11(c). These results are consistent with the analysis and simulation results presented above.

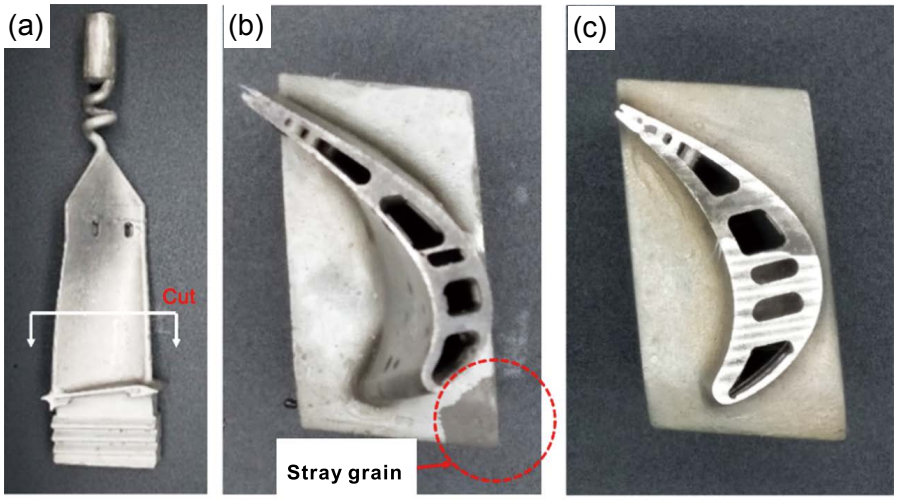

Fig. 11: Picture of blade casting showing the location of cutting (a), and section view of blade casting with traditional (b) and improved (c) moulds

In the DS process of the SC blade, after the process conditions, such as drawing rate, cooling temperature, etc, are determined, the mould structure is the only factor that affects heat dissipation during solidification. By changing the mould structure, the solidification thermal field can be improved to achieve good solidification quality. 3D printing technology can be used to flexibly fabricate any structure, which means that the mould design is no longer restricted by the die. The application of 3D printing technology to mould manufacturing can not only accelerate the fabrication of integral ceramic moulds containing cores but also flexibly change the external structure of the mould considering specific heat dissipation needs. The proposed mould baffle technology represents a new paradigm for eliminating the formation of stray strains in the platform.

5 Conclusions

Taking advantage of the flexibility of the IFTCM technology in mould making, an improved mould was fabricated using stereolithography and gelcasting technology to prevent the formation of stray grains in the blade platform. By adding a baffle under the mould platform, undercooling is reduced in the platform region, and the formation of the stray grains is prevented, as verified by means of a simulation and an experiment. The following conclusions are drawn:

(1) The thermal calculation result obtained using ProCAST software indicates that undercooling of the alloy melt in the platform region can be greatly reduced by using the improved mould; this would help avoid undercooling nucleation and eliminate stray grains. This effect is related to the baffle size: when the baffle outline size is 6 mm larger than the platform size, undercooling nucleation is eliminated, as confirmed by the results of the CAFE simulation.

(2) The formation of stray grains in the platform can be ascribed mainly to faster heat dissipation at the platform extremities than in the blade body. In the case of the traditional mould, the larger the platform size and the faster the drawing rate, the higher the probability of stray grain formation in the platform. By using the proposed mould baffle technology, however, the heat dissipation behavior in the platform can be

changed and therefore reduce undercooling of the alloy melt greatly; even when the platform size is large, the proposed mould baffle technology can help prevent the formation of stray grains successfully without a large reduction in the drawing rate.

(3) The results of the casting experiments prove that the blade has a good SC structure when using the improved mould, while the blade cast using the traditional mould has obvious stray grains in the platform.

(4) With the advantage of flexible manufacturing of shell mould structure by 3D printing, stray grains in the platforms of SC blades can be eliminated by adding a suitably sized baffle structure in the shell mould. This opens a window for optimizing the solidification temperature field of the blade through mould structure design.

Acknowledgements

This work was financially supported by the Industry-University Research Cooperation Project of Aero Engine Corporation of China (Grant No. HFZL2019CXY023), and the National Science and Technology Major Project (Grant No. 2017-VII-0008-0101).

References

[1] Reed R C. The superalloy fundamental and applications. Cambridge: Cambridge University Press, 2006: 1–10.
[2] Pollock T M, Tim S. Nickel-based superalloy for advanced turbine engines: Chemistry, microstructure, and properties. Journal of Propulsion and Power, 2006, 22(2): 358–361.
[3] Sims C T, Stoloff N S, Hagel W C. Superalloys II: High-temperature materials for aerospace and industrial power. New York: John Wiley and Sons, 1987: 1–23.
[4] Ma D and Bührig-Polaczek A. Avoiding grain defects in single crystal components by application of a heat conductor technique. International Journal of Materials Research, 2009, 100(8): 1145–1151.
[5] Ma D and Bührig-Polaczek A. Development of heat-conductor technique for single crystal components of superalloys. International Journal of Cast Metals Research, 2013, 22: 422–429.
[6] Ma D and Bührig-Polaczek A. Application of a heat conductor technique in the production of single crystal turbine blades. Metallurgical and Materials Transaction B, 2009, 40: 738–748.
[7] Meyer T V M, Dedecke D, Paul U, et al. Undercooling related casting defects in single crystal turbine blades. Superalloys, 1996: 471–479.
[8] Yang X L, Ness D, Lee P D, et al. Simulation of stray grain formation during single crystal seed melt-back and initial withdrawal in the Ni-base superalloy CMSX4. Materials Science & Engineering: A, 2005, 413–414: 571–577.
[9] Backman D G and Williams J C. Advanced materials for aircraft engine applications. Science, 1992, 255(5048): 1082–1087.
[10] Lu Z L, Zhao L, Li Y N, et al. Thermal behavior of integral Al_2O_3-based ceramic molds for fabricating gas turbine blades. Journal of Engineering Manufacture, 2014, 228(5): 695–703.
[11] Wu H, Li D R, Tang Y, et al. Rapid casting of hollow turbine blades using integral ceramic moulds. Journal of Engineering Manufacture, 2009, 223(6): 695–702.
[12] Tian G Q, Lu Z L, Miao K, et al. Formation mechanism of cracks during the freeze drying of gelcast ceramic parts. Journal of American Ceramic Society, 2015, 98(10): 3338–3345.
[13] Wu H H, Li D C, Tang Y, et al. Rapid fabrication of alumina-based ceramic cores for gas turbine blades by stereolithography and gelcasting. Journal of Materials Processing Technology, 2009, 209(18–19): 5886–5891.
[14] Cai K, Guo D, Huang Y, et al. Solid freeform fabrication of alumina ceramic parts through a lost mould method. Journal of European Ceramic Society, 2003, 23(6): 921–925.
[15] Young A C, Omatete O O, Janney M A, et al. Gelcasting of Alumina. Journal of American Ceramic Society, 1991, 74(3): 612–618.
[16] Neuer G. Spectral and total emissivity measurements of highly emitting materials. International Journal of Thermophysics,1995, 16(1): 257–265.
[17] Carter P, Cox D C, Gandin C A, et al. Process modelling of grain selection during the solidification of single crystal superalloy castings. Materials Science & Engineering: A, 2000, 280(2): 233–246.
[18] Chapman L A. Application of high temperature DSC technique to nickel based superalloys. Journal of Materials Science, 2004, 39(24): 7229–7236.
[19] Ma D, Wu Q, and Bührig-Polaczek A. Undercoolability of superalloy and solidification defects in single crystal components. Advanced Materials Research, 2011, 278: 417– 422.
[20] Ma D, Wang F, Wu Q, et al. Temperature evolution and grain defect formation during single crystal solidification of a blade cluster. China Foundry, 2017, 14(5): 456–460.
[21] Szeliga D, Kubiak K, Sieniawski J. Control of liquidus isotherm shape during solidification of Ni-based superalloy of single crystal platforms. Journal of Materials Processing Technology, 2016, 234(1): 18–26.